



# Stability of 8-hydroxyquinoline aluminum films encapsulated by a single Al<sub>2</sub>O<sub>3</sub> barrier deposited by low temperature atomic layer deposition

Tony Maindron<sup>a,\*</sup>, Jean-Yves Simon<sup>a</sup>, Emilie Viasnoff<sup>a</sup>, Dominique Lafond<sup>b</sup>

<sup>a</sup> CEA-LETI, MINATEC Campus, LETI/DOPT/SCOOP/Laboratoire des Composants pour la Visualisation, 17 rue des Martyrs, F-38054 Grenoble Cedex 9, France

<sup>b</sup> CEA-LETI, MINATEC Campus, LETI/DTSI/SCMC/, 17 rue des Martyrs, F-38054 Grenoble Cedex 9, France

## ARTICLE INFO

### Article history:

Received 19 March 2012

Received in revised form 10 July 2012

Accepted 12 July 2012

Available online 21 July 2012

### Keywords:

8-Hydroxyquinoline aluminum

Organic light emitting diode

Device stability

Atomic layer deposition

Encapsulation

Thin films

Diffusion barrier

## ABSTRACT

100 nm thick 8-AlQ<sub>3</sub> films deposited onto silicon wafers have been encapsulated by mean of low temperature atomic layer deposition of Al<sub>2</sub>O<sub>3</sub> (20 nm). Investigation of the film evolution under storage test as harsh as 65 °C/85% RH has been investigated up to ~1000 h and no severe degradation could be noticed. The results have been compared to raw AlQ<sub>3</sub> films which deteriorate far faster in the same conditions. For that purpose, fluorescence measurements and atomic force microscopy have been used to monitor the film evolution while transmission electron microscopy has been used to image the interface between AlQ<sub>3</sub> and Al<sub>2</sub>O<sub>3</sub>. This concept of bilayer AlQ<sub>3</sub>/Al<sub>2</sub>O<sub>3</sub> barrier films has finally been tested as an encapsulation barrier onto an organic light-emitting diode.

© 2012 Elsevier B.V. All rights reserved.

## 1. Introduction

8-Hydroxyquinoline aluminum (AlQ<sub>3</sub>) is being known for a long time in the world of organic light-emitting diodes (OLED). It has been reported as an electron transporting and emitting molecule in the first OLED-related publication from Kodak team in 1987. It is an organometallic compound of choice because it forms highly stable amorphous thin films by evaporation and possesses a high glass transition temperature (T<sub>g</sub>) of 165 °C. Its degradation processes have been studied for a long time and numerous papers reported on its photodegradation as well as on its reaction with water and/or oxygen to form non emissive by-products that act subsequently as fluorescent quenchers. Besides, when AlQ<sub>3</sub> acts as an electron-transporting material in an OLED, its main degradation comes from the instability of AlQ<sub>3</sub><sup>+</sup> species which degradation byproducts lead in general to a decrease of the OLED electroluminescence [1]. As AlQ<sub>3</sub> is a sensitive organic molecule, photooxidation and reaction with water could be prevented by a suitable isolation of the product in an inert atmosphere and a suitable encapsulation of the amorphous AlQ<sub>3</sub> films.

The concept of protection against oxidizing gas of atmosphere (H<sub>2</sub>O, O<sub>2</sub>) is mandatory for thin amorphous molecular films as well as for OLED. Usually, thin inorganic barrier layers are made of oxides, nitrides or oxynitrides usually deposited by low temperature PECVD and sputtering techniques [2]. Usually very low gas permeability

level, water vapor transmission rate (WVTR) around 10<sup>-6</sup> g/m<sup>2</sup>/day and oxygen transmission rate (OTR) around 10<sup>-3</sup> sccm/m<sup>2</sup>/day could be reached by building hybrid encapsulation stacks of the kind [organic/inorganic]<sub>n</sub>, n=4 on top of the device [3]. For that purpose, thick (~0.5–5 μm) vacuum deposited smoothing polymer layers are deposited between the thin mineral barrier layers (≤100 nm) which inevitably possess some intrinsic defects like pinholes or cracks. Their role is to decouple these defects from one barrier layer to another so that the paths for the oxidizing species to reach the fragile device are lengthened, and the whole degradation is delayed [4].

In order to decrease the number of decoupling organic layers and the thickness of barrier layers, very thin, conformal and almost “defect-free” barriers (with very low intrinsic OTR and WVTR), deposited at low temperatures (≤100 °C), must be used. The atomic layer deposition (ALD) technology really finds in that case its legitimacy and several groups have already reported the outperformance of ALD technology for barrier applications on OLED [5–10]. It is presumably because it is a thermal process that does not promote the formation of particles (plasma in PECVD or PVD tools does), as far as the cleanliness of the reactor itself is well mastered as well as the cleanliness of the device surface to be encapsulated.

Among all materials that can be deposited by mean of ALD technology, Al<sub>2</sub>O<sub>3</sub> turns out to be the candidate of choice. Its main features for encapsulation can be listed as follows: (i) large temperature process window (from room temperature to 250 °C) for reactive Al(CH<sub>3</sub>)<sub>3</sub> to make Al<sub>2</sub>O<sub>3</sub> films; (ii) films are homogeneous with a few defect density; (iii) the critical thickness is the lowest among

\* Corresponding author. Tel.: +33 601899745.

E-mail address: [tony.maindron@cea.fr](mailto:tony.maindron@cea.fr) (T. Maindron).

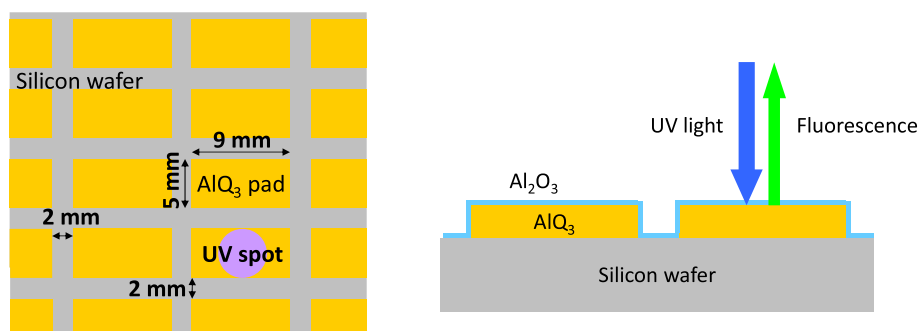


Fig. 1. (Left) Top view schematic of AlQ<sub>3</sub> pads on silicon and (right) cross section schematic of the AlQ<sub>3</sub> pads on silicon.

deposition techniques (ALD of Al(CH<sub>3</sub>)<sub>3</sub>/H<sub>2</sub>O is theoretically 2D growth and practically close to 2D growth), depending however upon the substrate surface; (iv) Al<sub>2</sub>O<sub>3</sub> ALD is transparent in the visible spectrum with good optical quality (emission of photons for top-emitting OLED is made through the top encapsulation); (v) good adhesion to substrate; and (vi) good coating chemistry [11].

The approach of this work has been motivated by the research for an encapsulation for OLED which was not based on usual polymeric decoupling layers but rather on molecular decoupling layers. Few examples of such molecular decoupling layers exist. Lee S.-N. et al. have described the use of the molecule 2-methyl-9,10-di(2-naphthyl)-anthracene (MADN) as a decoupling layer between sputtered SiN and SiON layers [12]. The authors explained that the integration of a MADN layer in the encapsulation stack can planarize the surface of the (n−1)th inorganic barrier layer before the deposition of the subsequent nth layer thus leading to lower pinhole density in the nth layer. The whole WVTR is thus reduced. Song et al. have integrated AlQ<sub>3</sub> films between evaporated LiF layers for the encapsulation of top-emitting OLED [13]. One of the main advantages of such molecular layers is that they are easily vacuum deposited so that the encapsulation process may potentially be fully integrated in the OLED fabrication line without any additional tool required for polymer deposition.

The deposition of Al<sub>2</sub>O<sub>3</sub> films from ALD of Al(CH<sub>3</sub>)<sub>3</sub>/H<sub>2</sub>O onto amorphous molecular films has been found however not to be an easy task. In this work, the AlQ<sub>3</sub> molecule has been found to be a material of choice for that purpose because it shows a high stability to the low temperature ALD of Al(CH<sub>3</sub>)<sub>3</sub>/H<sub>2</sub>O process. Two other molecular films of 4,7-diphenyl-1,10-phenanthroline (BPhen) and 2,2',7,7'-tetra(N, N-di-tolyl)amino-spiro-bifluorene (Spiro-TTB) have been also tested: they clearly react during the deposition process and crystallization of the organic layers appears clearly upon oxide deposition. With AlQ<sub>3</sub>, it has been possible to compare the stability of the single AlQ<sub>3</sub> films with Al<sub>2</sub>O<sub>3</sub> encapsulated AlQ<sub>3</sub> films versus time (up to ~1000 h) upon storage in a climatic environment as harsh as 65 °C/85% RH. To do that, the AlQ<sub>3</sub> and Al<sub>2</sub>O<sub>3</sub> films have been successively deposited onto silicon substrates and fluorescence measurements, atomic force microscopy (AFM) and transmission electron microscopy (TEM) analysis have been performed to monitor the evolution of the different AlQ<sub>3</sub> films upon storage time and to characterize the interface between the organic and inorganic films. At the end, we will show that the concept of OLED thin film encapsulation based on this bilayer

barrier AlQ<sub>3</sub>/Al<sub>2</sub>O<sub>3</sub> can improve a single Al<sub>2</sub>O<sub>3</sub> thin film encapsulation for OLED.

## 2. Experimental details

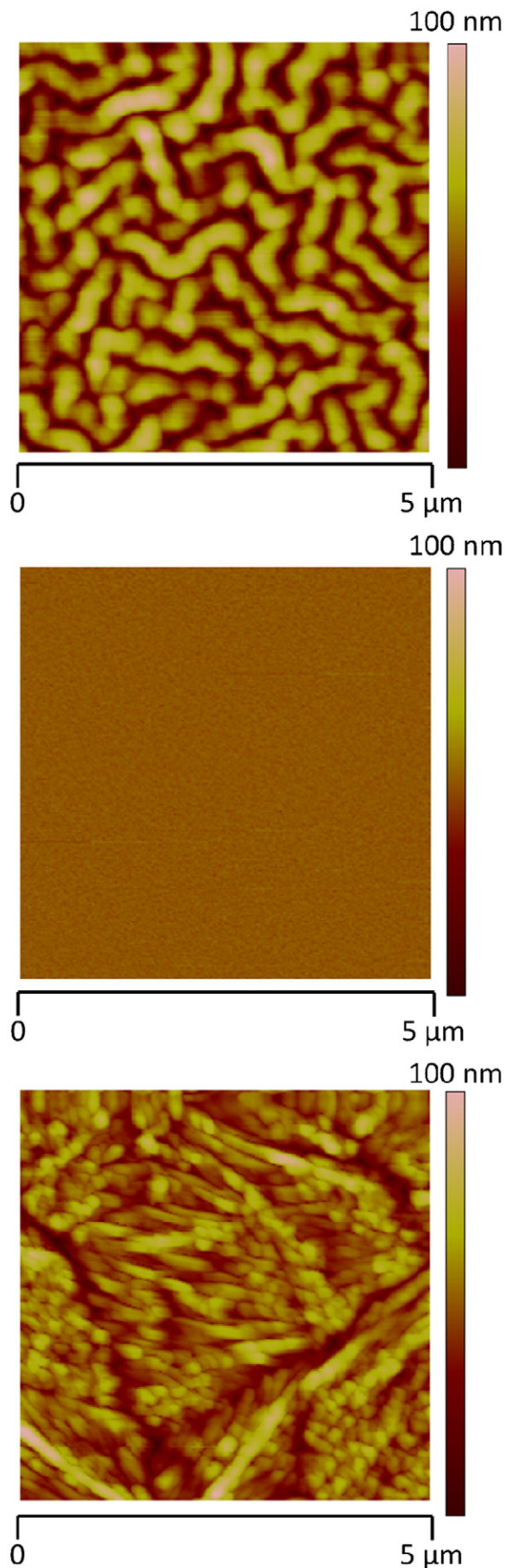
AlQ<sub>3</sub> films as well as BPhen and Spiro-TTB have been deposited onto 200 mm silicon wafers by vacuum deposition. The whole process took place in a clean room environment and the evaporation tool was a cluster tool Sunicell Plus 200 from Sunic Systems. The clean silicon wafers have been used as received. Once introduced inside the cluster tool, the silicon wafers were Ar-plasma treated (60 W, 60 s). The base pressure in the deposition chamber was  $1 \times 10^{-7}$  Torr. The evaporation rate of the organic compounds was ~0.1 Å/s. The deposition has been performed through a shadow mask to allow ~135 pads of organic molecule (~9×5 mm<sup>2</sup> each) to be deposited independently onto the silicon wafer. The organic layer thickness was controlled by a quartz crystal monitor and was cross-checked by ex situ profilometer measurement. The silicon wafers with the organic pads were stored into a N<sub>2</sub> filled glove box from MBraun (UniLab model) directly connected to the Sunicell system and then transferred to a Savannah 200 ALD system from Cambridge Nanotech hermetically embedded in another UniLab glove box system. The whole process took place in an inert atmosphere because clean transfer inert boxes were used for that purpose. The ALD process has been performed at 85 °C, in a Savannah 200 from Cambridge Nanotech, from Al(CH<sub>3</sub>)<sub>3</sub>/H<sub>2</sub>O precursors at a growth per cycle of 0.85 Å/cycle. Prior to deposition, the silicon wafer with organic pads onto it has been allowed to degas for 1800 s inside the ALD chamber. The first precursor to be pulsed during the ALD run was H<sub>2</sub>O. Right after the ALD run, the substrate containing the organic pads and Al<sub>2</sub>O<sub>3</sub> overcoatings have been inspected inside the glove box before evacuation to the laboratory breathable atmosphere.

The storage of the wafer containing the AlQ<sub>3</sub> pads has been done in a climatic test chamber from Votsch. The conditions have been fixed to 65 °C/85% RH during the entire test. Comparative study was performed by storing a reference sample in the laboratory atmosphere, at 22 °C/50% RH. The climatic chamber was totally dark while the storage in the lab took place in a shaded place.

Fluorescent measurements have been performed by using a UV–VIS broadband Hg lamp (350 mW/cm<sup>2</sup> at surface) connected to an Olympus BX51 optical microscope which allows the excitation of AlQ<sub>3</sub> films with the UV part only of the lamp and the large band observation in the visible (fluorescent peak of AlQ<sub>3</sub> film is ~532 nm). Fluorescence (FL) spectra of AlQ<sub>3</sub> films have been recorded by using a PR655 spectrophotometer from Photo Research head-mounted onto the optical microscope. In order to ensure a good reproducibility of the fluorescent measurements, the same settings for the measurements have been applied each time onto the microscope as well as the ambient lighting in the laboratory. The UV lamp has been used only for that purpose during the whole period of testing. Its aging is thus not of concern in this work. The measurements have been performed onto middle pads to avoid dispersion due to the AlQ<sub>3</sub> thickness variation on the whole 200 mm silicon

**Table 1**  
Description of molecules encapsulated with Al<sub>2</sub>O<sub>3</sub> ALD.

Molecule	BPhen	Spiro-TTB	AlQ <sub>3</sub>
T <sub>g</sub> (°C)	65	149	165
Si/molecule (100 nm)/Al <sub>2</sub> O <sub>3</sub> (ALD, 20 nm)	Reacts (crystallization)	Reacts (crystallization)	Highly stable



wafer. 20 pads have been chosen randomly each time to ensure a good statistical characterization. The  $\times 10$  objective has been selected each time so that the light beam spot surface (radius is 2.5 mm), at focus, was entirely localized inside the AlQ<sub>3</sub> pad to be excited. Ratio of surfaces is  $(9 \times 5) / (\pi \times 2.5^2) \sim 2.3$ . Fig. 1 explained the detail of the experimental design of AlQ<sub>3</sub> pads and their fluorescent measurement.

AFM measurements have been performed with an AFM Dimension 3100 from Veeco. The contact mode has been employed for that purpose. Each new session with the AFM has been calibrated by using a calibration Au grid with predefined patterns. The AFM tool has been used to evaluate the roughness (Rq, nm) and make the surface imaging of the different films studied in this work. The error on the roughness corresponds to the standard deviation of a population of 5 Rq measurements on the same pad. The different images have been all post treated in the same manner on the AFM software. TEM has been performed with a JEOL JEM 2010FEF operating at 200 kV. An in column omega-type energy filter was used with a 10 eV slit for elastic electrons imaging (EFTEM mode). The 100 nm thick TEM lamella has been prepared using a focus ion beam FEI STRATA DB-400 with 30 kV gallium ions for coarse milling and 5 kV for final cleaning process.

The OLED stack described in this work consists of white PIN structures [14]. The OLED architecture comprises a p-doped hole transporting layer next to the highly reflective anode made onto a silicon wafer, an emitting system sandwiched in between an electron blocking layer and a hole blocking layer, and an n-doped electron transporting layer next to the semi-transparent cathode. An additional high optical index capping layer has been deposited onto the cathode surface. The evolution of a thin-film OLED encapsulated in 65 °C/85% RH storage conditions has been recorded as followed (Fig. 7): the y axis represents the percentage of diodes with less than 1% of dark spots onto their emitting surface. The x axis represents the time spent at 65 °C/85% RH. A reference OLED, that uses a single 20 nm thick Al<sub>2</sub>O<sub>3</sub> ALD layer, has been added for comparison. The statistical analysis has been performed onto 135 diodes (9 × 5 mm<sup>2</sup>). The photo acquisition has been made onto a fully automated prober tool (TEL P-8XL) by mean of a high resolution digital camera (Nikon D700). Once captured, the 135 images of the OLED, all biased at the same voltage, have been processed with an image processing software. The color depth of the image has been then decreased down to 2 binary colors so that the procedure allowed the evaluation of the number of dark pixels onto the total number of pixels.

### 3. Results and discussion

#### 3.1. Stability of different organic molecular films upon Al<sub>2</sub>O<sub>3</sub> ALD deposition

It is well recognized that a high T<sub>g</sub> character is beneficial to the stability of organic semiconductors [15]. Numerous publications have for instance reported about the crystallization of low T<sub>g</sub> TPD molecules (65 °C) upon heating [16]. As a consequence, the ALD deposition onto small molecules from H<sub>2</sub>O precursor, and to some extent from highly reactive precursor like Al(CH<sub>3</sub>)<sub>3</sub>, at temperature of 85 °C, does not appear to be a natural task. First, two molecules have been tested in our lab, namely BPhen and Spiro-TTB which are well-known conjugated small molecules in the OLED world [17,18]. As the T<sub>g</sub> of BPhen and Spiro-TTB differ radically, 65 °C and 149 °C respectively, we were inferring that the T<sub>g</sub> of the molecular compounds may play a role in their stability against Al(CH<sub>3</sub>)<sub>3</sub>/H<sub>2</sub>O chemistry during the ALD process. Unfortunately, both compounds have shown a reaction against the ALD process leading to obvious crystallization of the films. On the contrary, AlQ<sub>3</sub> (T<sub>g</sub> = 165 °C) films

Fig. 2. AFM surface images of (top) Si/BPhen (100 nm)/Al<sub>2</sub>O<sub>3</sub> (20 nm), (middle) Si/AlQ<sub>3</sub> (100 nm)/Al<sub>2</sub>O<sub>3</sub> (20 nm) after Al<sub>2</sub>O<sub>3</sub> deposition and (bottom) Si/AlQ<sub>3</sub> after t + 12 h at 65 °C/85% RH.

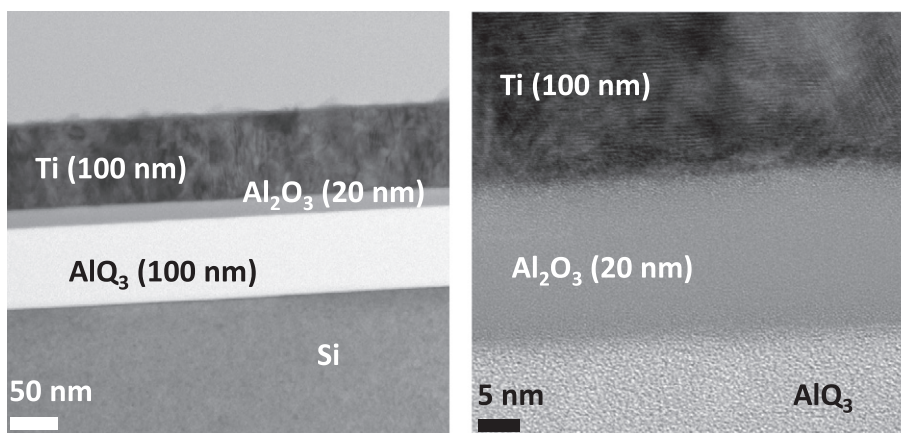


Fig. 3. TEM cross section of Si/AIQ<sub>3</sub> (100 nm)/Al<sub>2</sub>O<sub>3</sub> (20 nm) at 2 different scales.

behave very nicely and the Al<sub>2</sub>O<sub>3</sub> film could be deposited upon it without any observable sign of degradation (see Table 1 for comparison).

Fig. 2 depicts the top surface imaging of a film of Si/Bphen (100 nm)/Al<sub>2</sub>O<sub>3</sub> (20 nm) compared to Si/AIQ<sub>3</sub> (100 nm)/Al<sub>2</sub>O<sub>3</sub> (20 nm). The R<sub>q</sub> of the surface of 100 nm unencapsulated BPhen films deposited onto silicon wafers is  $3.670 \pm 0.115$  nm as measured by AFM in a standard atmosphere (less than 2 h after exit of sample from glove box). It can be seen on the other hand that a rough surface of BPhen/Al<sub>2</sub>O<sub>3</sub> has been obtained after the deposition of the oxide from ALD at 85 °C. Its R<sub>q</sub> is  $20.45 \pm 2.61$  nm, a value close to R<sub>q</sub> values measured for crystallized Bphen films onto glass substrates [19]. For comparison, an Al<sub>2</sub>O<sub>3</sub> film onto the Si surface shows a low R<sub>q</sub> of  $0.442 \pm 0.172$  nm. Films of Spiro-TTB also crystallized upon oxide deposition from ALD of Al(CH<sub>3</sub>)<sub>3</sub>/H<sub>2</sub>O at 85 °C. Their R<sub>q</sub> values have not been measured but the crystallization is easily observable by

means of an optical microscope. Some internal tests have shown that the use of ozone as oxidant could avoid the crystallization of Spiro-TTB. Therefore, this may suggest that the residence time of water molecules, which are longer than ozone molecules to be purged out at 85 °C [20], in the reaction chamber and onto the organic surface is long and may play a role in the crystallization of the organic Spiro-TTB layer. For BPhen films, the deposition temperature during ALD process being 25 °C higher than the molecule T<sub>g</sub>, this could explain the crystallization of BPhen which has a severe tendency to crystallize by itself because of high molecular motion of molecules [21]. The unencapsulated films of BPhen deposited onto the silicon wafers crystallized after a couple of days in our laboratory. Therefore, the crystallization of BPhen films upon ALD of Al<sub>2</sub>O<sub>3</sub> must have been accelerated by the severe conditions of deposition. For Spiro-TTB, the temperature argument cannot explain by itself the reaction that leads to crystallization of the film because the T<sub>g</sub> of Spiro-TTB is higher than the deposition temperature in the ALD reactor. Moreover, unencapsulated Spiro-TTB films deposited onto Si wafers did not show any crystallization for months in our laboratory atmosphere. Hence, for this molecule, an unfavorable reaction to the ALD precursors, Al(CH<sub>3</sub>)<sub>3</sub> or H<sub>2</sub>O must have occurred. On the contrary, the surface of AIQ<sub>3</sub>/Al<sub>2</sub>O<sub>3</sub> remains a very smooth surface after the oxide deposition and R<sub>q</sub> values as low as  $1.169 \pm 0.077$  nm have been measured. This is slightly higher to the R<sub>q</sub> value of unencapsulated AIQ<sub>3</sub> films onto silicon which has been measured to be  $0.358 \pm 0.152$  nm. These observations clearly indicate that the T<sub>g</sub> criterion is not the only parameter to be considered if ALD of Al<sub>2</sub>O<sub>3</sub> from Al(CH<sub>3</sub>)<sub>3</sub>/H<sub>2</sub>O is to be experienced onto organic molecular films at 85 °C. As AIQ<sub>3</sub> films were the only ones to survive the ALD process, the following development has thus been focused only on this material and has allowed the investigation of the stability of Al<sub>2</sub>O<sub>3</sub>-encapsulated AIQ<sub>3</sub> films versus raw AIQ<sub>3</sub> films.

### 3.2. TEM imaging of AIQ<sub>3</sub>/Al<sub>2</sub>O<sub>3</sub> interface

TEM imaging allowed the making of the cross section at very high resolution of the interface AIQ<sub>3</sub>/Al<sub>2</sub>O<sub>3</sub>. From Fig. 3 it can be seen that the interface is very sharp and that the oxide had apparently grown in a real ALD mode, 2D mode, and close manner. Note that the Ti top layer has been added to the original stack to enhance the contrast for TEM observation. It is well-known for polymers that the ALD coating microstructure as well as the interface characteristics strongly depends on the starting organic polymer composition. As a result, Al(CH<sub>3</sub>)<sub>3</sub> diffusion into the polymer matrix could appear and subsurface growth of Al<sub>2</sub>O<sub>3</sub> ALD has been observed onto –OH rich polymers [22]. For molecular films, this kind of behavior may be also valid. For AIQ<sub>3</sub> films, it can be seen from these high resolution images that the oxide layer is amorphous and that the interface between Al<sub>2</sub>O<sub>3</sub> and

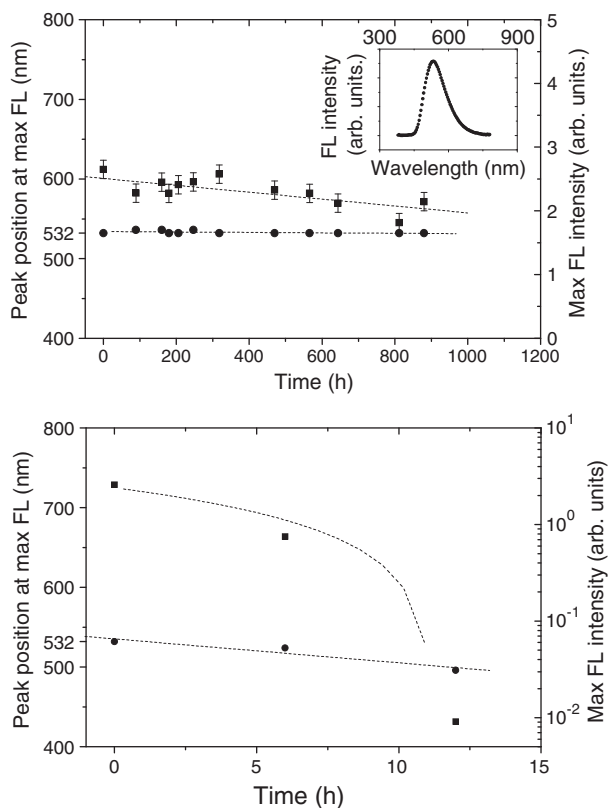


Fig. 4. FL peak position at maximum FL intensity (filled circles) and maximum FL intensity (filled squares) for (top) Si/AIQ<sub>3</sub> (100 nm)/Al<sub>2</sub>O<sub>3</sub> (20 nm) – inset: FL spectrum of Si/AIQ<sub>3</sub>/Al<sub>2</sub>O<sub>3</sub> at t<sub>0</sub> and (bottom) Si/AIQ<sub>3</sub> (100 nm) versus storage time at 65 °C/85% RH.

**Table 2**  
Description of storage conditions and fit model for virgin AlQ<sub>3</sub> films and AlQ<sub>3</sub> films encapsulated with Al<sub>2</sub>O<sub>3</sub> ALD.

	Storage conditions	Storage time $t_f$ (h)	$\frac{I_{FL}(t_f)}{I_{FL}(0)}$	Best fit <sup>b</sup>
Si/AlQ <sub>3</sub>	65 °C/85% RH	12	$3.5 \times 10^{-3a}$	–
Si/AlQ <sub>3</sub>	22 °C/50% RH	1130	0.08	$I_{FL}(t) = 0.0214 \times e^{-0.12641 \times t^{0.4122}}$
Si/AlQ <sub>3</sub> /Al <sub>2</sub> O <sub>3</sub>	65 °C/85% RH	889	0.79	$I_{FL}(t) = 0.0254 - 6.10^{-6} \times t$

<sup>a</sup> Obvious crystallization of AlQ<sub>3</sub> film.

<sup>b</sup> Right y axis "Max FL intensity (arb. units)" on Figures 4, 5 and 6 have been multiplied by 100 for clarity – equation fits have been performed onto original values.

AlQ<sub>3</sub> is rather sharp and smooth with apparently no obvious image contrast on the top AlQ<sub>3</sub> film close to the oxide coating. This suggests that there is no subsurface growth of the oxide in the organic film due to precursor diffusion inside the organic matrix. As BPhen and Spiro-TTB films have been crystallized, it was unfortunately not possible to compare Al<sub>2</sub>O<sub>3</sub> ALD growth onto different molecular surfaces. This behavior is however under investigation in our laboratory and other stable molecular compounds are being sought for that purpose.

### 3.3. Comparison of evolution of AlQ<sub>3</sub> films and Al<sub>2</sub>O<sub>3</sub> encapsulated AlQ<sub>3</sub> films upon storage

Storage of Si/AlQ<sub>3</sub> and Si/AlQ<sub>3</sub>/Al<sub>2</sub>O<sub>3</sub> films has been performed at 65 °C/85% RH. The results have been depicted in Fig. 4 where the FL peak position at maximum FL intensity of AlQ<sub>3</sub> and the maximum FL intensity have been plotted versus storage time. Table 2 reported also the different characteristics of the storage conditions and related performances of the different films. The results clearly indicate that the raw AlQ<sub>3</sub> film does not withstand the severe climatic conditions. The films crystallized in less than 15 h leading to an obvious FL quenching as well as to a FL blue shift from 532 nm to 496 nm. This blue shift of 36 nm reveals that the crystalline form of AlQ<sub>3</sub> in that case is presumably the  $\delta$ -phase ( $\delta$ -AlQ<sub>3</sub>) of the molecule as described by Cölle et al. [23]. On the contrary, the AlQ<sub>3</sub> film protected from atmosphere by the 20 nm thick oxide layer showed an incredible stability up to 889 h. As a result, the FL peak at 532 nm remains unchanged and the FL intensity decreases by ~20% with a linear behavior (see Table 2). No crystallization could be observed at the end. AFM roughness measurement gave an Rq value of  $2.261 \text{ nm} \pm 0.260 \text{ nm}$  higher than the initial value. As Al<sub>2</sub>O<sub>3</sub> films are known to react with moisture to form Al(OH)<sub>x</sub> hydrated compounds, as described by Dameron et al. for Al<sub>2</sub>O<sub>3</sub> low temperature deposited ALD films [24], it is reasonable to assume that the surface roughness increased by 93% is a consequence of the exposition of the oxide layer to the high humidity level during the whole storage test. As the storage conditions of 65 °C/85% RH revealed to be too harsh for the raw AlQ<sub>3</sub> films which deteriorate too quickly to enable any comparison with

encapsulated AlQ<sub>3</sub> films, additional experiments have been performed at 22 °C/50% RH on Si/AlQ<sub>3</sub> films. Fig. 5 represents the evolution of fluorescence intensity and peak at maximum intensity versus time at 22 °C/50% RH of Si/AlQ<sub>3</sub> up to 1130 h. It turns out that the organic films remain amorphous and no obvious crystallization could be detected nor by optical inspection or by AFM imaging. This is not surprising because AlQ<sub>3</sub> film structures are known to remain stable in the atmosphere for years [25]. Fig. 6 emphasizes onto FL spectra (linear-log scale) of the different AlQ<sub>3</sub>-based samples before and after storage. It could be seen that the FL peak at maximum does not change for the Si/AlQ<sub>3</sub> sample stored at 22 °C/50% RH for 1130 h. However its evolution of the FL intensity upon time at 22 °C/50% RH behaves differently compared to Si/AlQ<sub>3</sub>/Al<sub>2</sub>O<sub>3</sub> at 65 °C/85% RH (Table 2). A stretch exponential decay of the form

$$I_{FL}(t) = I_{FL}(0) \times e^{-\alpha t^\beta},$$

where  $I_{FL}(0)$  corresponds to the initial FL intensity while  $\alpha$  and  $\beta$  are fitting parameters, could be applied to the data with excellent correlation coefficients. This exponential decrease has been ascribed to the moisture ingress on AlQ<sub>3</sub> molecules as reported by former studies [26]. Degradation phenomenon that occurs in the AlQ<sub>3</sub> molecules has been extensively studied and it is well recognized today that the AlQ<sub>3</sub> monomer reacts with H<sub>2</sub>O molecules which firstly hydrolyses the AlQ<sub>3</sub> monomer in the form of an 8-hydroxyquinoline monomer that subsequently reacts with the byproduct monomers together with O<sub>2</sub> to form a dark, non-emissive polymer [27]. In our work, as the AlQ<sub>3</sub> film protected from H<sub>2</sub>O and O<sub>2</sub> by the single Al<sub>2</sub>O<sub>3</sub> ALD oxide layer shows a very slight decrease of FL intensity (only ~20% loss after 889 h at 65 °C/85% RH), it has been thus clearly demonstrated that the single Al<sub>2</sub>O<sub>3</sub> acts as a very good barrier. Further analyses are going to be conducted in our lab to better understand the properties of the AlQ<sub>3</sub>/Al<sub>2</sub>O<sub>3</sub> interface as well to investigate the structure evolution of the encapsulated AlQ<sub>3</sub>.

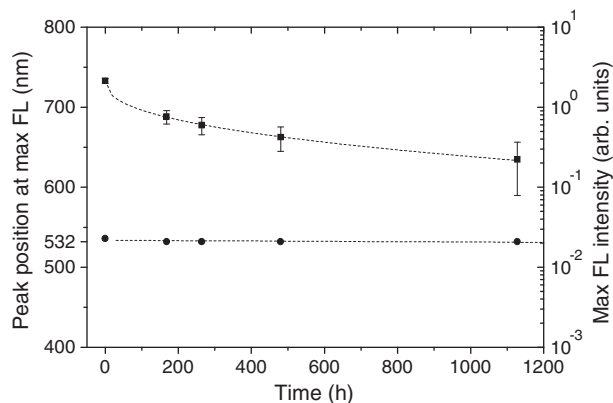


**Fig. 5.** FL peak position at maximum FL intensity (filled circles) and maximum FL intensity (filled squares) for Si/AlQ<sub>3</sub> (100 nm) versus storage time at 22 °C/50% RH.

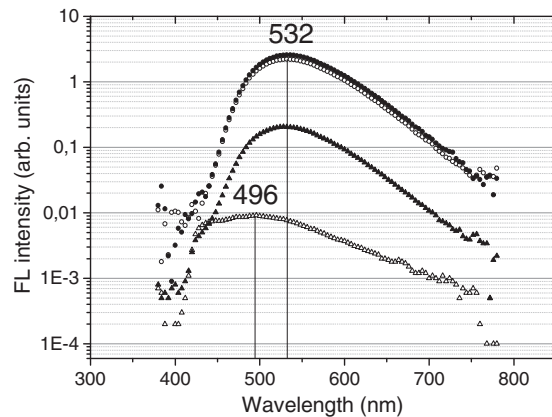


**Fig. 6.** FL spectra (linear-log) of Si/AlQ<sub>3</sub>/Al<sub>2</sub>O<sub>3</sub> at  $t_0$  (filled circles), at  $t+889$  h in 65 °C/85% RH storage conditions (opened circles), of Si/AlQ<sub>3</sub> at  $t+1130$  h in 22 °C/50% RH storage conditions (filled triangles) and of Si/AlQ<sub>3</sub> at  $t+12$  h in 65 °C/85% RH storage conditions (opened triangles).

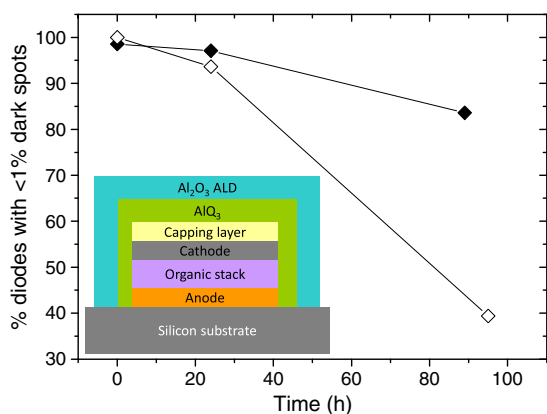


**Fig. 7.** Evolution of an OLED encapsulated with AlQ<sub>3</sub>/Al<sub>2</sub>O<sub>3</sub> (filled diamonds) – inset: illustration of the device – and evolution of a reference OLED encapsulated with a single Al<sub>2</sub>O<sub>3</sub> ALD layer (opened diamonds) versus storage time at 65 °C/85% RH.

### 3.4. OLED encapsulation by AlQ<sub>3</sub>/Al<sub>2</sub>O<sub>3</sub> bilayer

As these developments could be somewhat related to thin film encapsulation of OLED and their related performances, we tested this bilayer AlQ<sub>3</sub>/Al<sub>2</sub>O<sub>3</sub> as a thin film barrier for an OLED and compared it to a single Al<sub>2</sub>O<sub>3</sub> encapsulated OLED in 65 °C/85% RH storage conditions. Results have been depicted onto Fig. 7. The assumption made here is that a dark pixel stands for a dark spot which reveals to be experimentally true. It can be seen that the bilayer AlQ<sub>3</sub>/Al<sub>2</sub>O<sub>3</sub> encapsulated OLED has more than 80% of diodes with less than <1% of dark spots after ~100 h. In comparison, the reference diode has less than 40% of diodes with less than <1% of dark spots after ~100 h. This clearly shows that the dark spot appearance and growth are delayed by the presence of the bilayer AlQ<sub>3</sub>/Al<sub>2</sub>O<sub>3</sub> encapsulating stack. The total number of dark spots is also reduced with the bilayer stack compared to the single Al<sub>2</sub>O<sub>3</sub> barrier.

## 4. Conclusions

In summary, it has been shown that low temperature ALD (85 °C) of Al<sub>2</sub>O<sub>3</sub> films from Al(CH<sub>3</sub>)<sub>3</sub> and H<sub>2</sub>O could be implemented onto organic molecular films like AlQ<sub>3</sub>. The oxide film shows very good barrier properties allowing a highly reliable encapsulation of the AlQ<sub>3</sub> films. However, the deposition of Al<sub>2</sub>O<sub>3</sub> films from Al(CH<sub>3</sub>)<sub>3</sub> and H<sub>2</sub>O onto organic molecular films has been shown to be a tricky job because molecules like BPhen or Spiro-TTB clearly crystallized upon the process. It turns out that the intrinsic nature of the molecule to be encapsulated rather than its T<sub>g</sub> seems to play a role in the observed stability. The fluorescence decrease of encapsulated AlQ<sub>3</sub> films has been measured to be ~20% after 889 h at 65 °C/85% RH with a linear regression. On the contrary, the unencapsulated organic films crystallize under these harsh conditions of storage while their aging in

standard atmosphere (22 °C/50% RH) follows an exponential decrease of the fluorescence intensity down to 90% after 1130 h but without any crystallization. As expected, the aging mechanisms of AlQ<sub>3</sub> films are thus different between the raw films and the Al<sub>2</sub>O<sub>3</sub>-encapsulated ones. Some investigations (FTIR and TOF-SIMS analyses) are under development in our laboratory to understand the degradation mechanisms of the low temperature ALD Al<sub>2</sub>O<sub>3</sub>-encapsulated AlQ<sub>3</sub> films.

## Acknowledgment

The authors would like to thank the European Commission for the financial support through the European project (FP7) SCOOP.

## References

- [1] A. Hany, Z.D. Popovic, Chem. Mater. 16 (2004) 4522.
- [2] H.K. Kim, M.S. Kim, J.-K. Kang, J.-J. Kim, M.-S. Yi, Appl. Phys. Lett. 90 (2007) 013502.
- [3] P.E. Burrows, L.G. Graff, M.E. Gross, P.M. Martin, M.K. Shi, M. Hall, E. Mast, C. Bonham, W. Bennett, M.B. Sullivan, Displays 22 (2001) 65.
- [4] J.D. Affinito, M.E. Gross, C.A. Coronado, G.L. Graff, L.N. Greenwell, P.M. Martin, Thin Solid Films 290–291 (1996) 63.
- [5] S.-H.K. Park, J. Oh, C.-S. Hwang, J.-I. Lee, Y.S. Yang, H.Y. Chu, Electrochem. Solid-State Lett. 8 (2005) H21.
- [6] S.J. Yun, Y.-W. Ko, J.W. Lim, Appl. Phys. Lett. 85 (2004) 4896.
- [7] J. Meyer, D. Schneidenbach, T. Winkler, S. Hamwi, T. Weimann, P. Hinze, S. Ammermann, H.-H. Johannes, T. Riedl, W. Kowalski, Appl. Phys. Lett. 94 (2009) 233305.
- [8] P. Mandlik, J. Gartside, L. Han, I.-C. Cheng, S. Wagner, J.A. Silvermail, R.-Q. Ma, M. Hack, J.J. Brown, Appl. Phys. Lett. 92 (2008) 103309.
- [9] Y.G. Lee, Y.-H. Choi, Org. Electron. 10 (2009) 1352.
- [10] A.P. Ghosh, L.J. Gerenser, C.M. Jarman, J.E. Fornalik, Appl. Phys. Lett. 86 (2005) 223503.
- [11] R.L. Puurunen, J. Appl. Phys. 97 (2005) 121301.
- [12] S.-N. Lee, S.-W. Hwang, C.H. Chen, Jpn. J. Appl. Phys. 46 (2007) 7432.
- [13] S. Liu, D. Zhang, Y. Li, L. Duan, G. Dong, L. Wang, Y. Qiu, Chin. Sci. Bull. 53 (2008) 958.
- [14] T. Maindron, M.B. Khalifa, D. Vaufrey, H. Cloarec, C. Pinot, H. Doyeux, J.C. Martinez, S. Cina, SID Int. Symp. Dig. Tech. 37 (2006) 1189.
- [15] F. Santerre, I. Bedja, J.P. Dodelet, Y. Sun, J. Lu, A.S. Hay, M. D'Iorio, Chem. Mater. 13 (2001) 1739.
- [16] M. Nagai, H. Nozoye, J. Electrochem. Soc. 154 (2007) J239.
- [17] S. Scholz, Q. Huang, M. Thomschke, S. Olthof, P. Sebastian, K. Walzer, K. Leo, S. Oswald, C. Corten, D. Kuckling, J. Appl. Phys. 104 (2008) 104502.
- [18] T.P.I. Saragi, T. Fuhmann-Lieker, J. Salbeck, Adv. Funct. Mater. 16 (2006) 966.
- [19] S.-Y. Chen, T.-Y. Chu, J.-F. Chen, C.-Y. Su, C.H. Chen, Appl. Phys. Lett. 89 (2006) 053518.
- [20] S.K. Kim, S.W. Lee, C.S. Hwang, Y.-S. Min, J.Y. Won, J. Jeong, J. Electrochem. Soc. 153 (2006) 1.
- [21] Y. Masumoto, T. Mori, Thin Solid Films 516 (2008) 3350.
- [22] J.C. Spagnola, B. Gong, S.A. Arvidson, J.S. Jur, S.A. Khan, G.N. Parsons, J. Mater. Chem. 20 (2010) 4213.
- [23] M. Cölle, W. Brütting, Phys. Status Solidi B 6 (2004) 1095.
- [24] A.A. Dameron, S.D. Davidson, B.B. Burton, P.F. Garcia, R.S. McLean, S.M. George, J. Phys. Chem. C 112 (2008) 4573.
- [25] E.-M. Han, L.-M. Do, N. Yamamoto, M. Fujihira, Thin Solid Films 273 (1996) 202.
- [26] G. Baldacchini, T. Baldacchini, A. Pace, R.B. Podes, J. Electrochem. Soc. 151 (2004) H93.
- [27] F. Papadimitrakopoulos, X.-M. Zhang, D.L. Thomsen, K.A. Higginson, Chem. Mater. 8 (1996) 1363.